RoboBoat 2026: Technical Design Report

Abdelrhman, Abdullah, Karim, Shehabeldin, Ahmed, and Mohamed

Military Technical College, Egypt

Abstract– MW is debuting the Mandjet autonomous surface vehicle at RoboBoat 2026. Following our appearance last season, we faced the challenge of building a more reliable, modular, and well-integrated platform, and we plan to attempt every task at the competition. While our team has prepared for all tasks, we prioritized navigation challenges to ensure reliable maneuverability and navigation, with a strong emphasis on hull design and communication systems before expanding our focus to other tasks. Our strategy emphasizes adaptability and reliability to create a well-functioning system that serves as a foundation for future development and improvements. In keeping with our commitment to demonstrate new promise this season, we improved overall system integration, and our testing process has been thorough across multiple environments to ensure reliable performance.

I. Competition Strategy

This season, our goal is to present a vehicle that offers mechanical resilience alongside a well-integrated system of electrical and software components. With this in mind, our objective is to attempt every task in the competition; however, we have prioritized refining our detection model. Guided by this strategy, we focused on detection-related tasks (Tasks 1, 2, 3, and 4) to improve our existing vision model. Tasks 5 and 6, on the other hand, have been given lower priority. This decision was made after evaluating our capabilities and hardware requirements, as we chose to focus on achieving consistent performance before addressing more complex systems.

A. Environment

From our previous participation in RoboBoat, we gained valuable knowledge about the environmental conditions at Nathan Benderson Park which present a significant challenge due to increased wave activity and elevated wind speeds specially in this time of the year. So, we took careful consideration of stability and that what we considered during the mechanical design process.

B. Task Completion

1) Task (1,2,3,4):

The Mandjet can identify the locations of red and green buoy gates while maintaining a safe distance to avoid collisions. Buoy colors and numbers are detected, and their locations and timestamps are recorded, which supports reliable detection and maneuverability for Tasks 1 and 2.

For Task 3, our YOLO model has been trained and refined to detect the Solid colored cylinder in order to determine the direction of rotation, while also recording its color. Lastly, successful execution of Task 4 requires the implementation of two dedicated mechanical systems.

The racquetball shooter uses a flywheel mechanism consisting of two high-speed, counter-rotating wheels that launch the ball. For the yellow vessels, we installed a water pump beneath the boat that shoots water from its muzzle once a yellow vessel is detected.

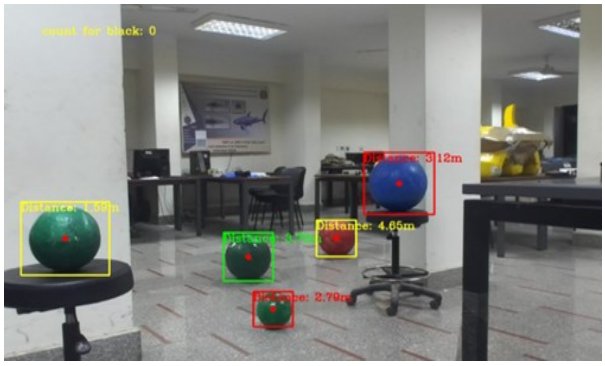

Figure 1: Red, green and blue buoys detected by ourYOLOv4 model.

To ensure high-precision aiming, we use the ZED camera to calculate the distance between the boat and the vessel, allowing us to compute the projectile trajectory. The mechanism is activated only when the vessel is detected and within range, which guarantees high accuracy.

2) Task (5,6):

We chose these tasks to be lower on our priority list due to the additional hardware and increased complexity of their requirements; nonetheless, we aim to attempt all tasks. This year, the docking task approach has changed due to the use of Solid colored cylinder that indicate the availability of each dock.

By training our model to detect its colors, the system records the cylinder color through a dedicated ROS node, which also receives and compares the numerical indicators. Another node subscribes to this data, and once the lowest number and the correct cylinder color are detected, the docking sequence is initiated. When the Mandjet begins the docking procedure, small adjustments to thruster values are made, guided by ZED camera distance measurements from the dock, to ensure accurate docking without collisions.

We faced several challenges in detecting the required frequencies and tuning the model to respond once a specific frequency is identified. One of our main concerns is noise interference leading to false detections. To address this, we implemented a ±5% tolerance around the specified frequencies. This tolerance window balances sensitivity and robustness, reducing false negatives while avoiding false positives.

II. Design Strategy

Our strategy is developed based on learn from what we had to face in our RoboBoat participation, in our previous design insufficient freeboard take it to make our boat overturns and sink in water, based on this experience our mechanical team focused on improving freeboard waterline height and overall buoyancy to enhance stability and survivability in rough environmental conditions.

A. Hulls

For the ASV Mandjet, a catamaran hull type was selected to maximize transverse stability and reduce hydrodynamic drag when compared to a monohull design. This configuration improved resistance to roll motion and enhances operational reliability in wave and wind affected environments.

The hulls were manufactured using fiberglass composite material, chosen for its favorable strength-to-weight ratio, corrosion resistance in freshwater environments, and suitability for complex hull geometries. Each hull has a mass of approximately 5.5 kg and is capable of supporting a payload of up to 33 kg, providing sufficient buoyancy for onboard systems while maintaining structural integrity.

Our boat features a freeboard ranging between 10 cm and 15 cm, which increasing the waterline height respect to previous design which was between 7 cm to 8 cm by 25% at least and approximately 40-100%. Significantly improving wave-handling capability and reducing the risk of water ingress.

B. Waterproofing

Our strategy focuses on preventing water ingress by protecting sensitive electronics and ensuring no leakage occurs inside the hulls.

C. Shooting mechanism

We decided to design a launching system that includes a primary inclined tube, holding three balls. Following that, the launching stage which have a servo motor rise the ball up from the tube and push it to a rail that leading to two high-speed servos that make direct contact with the ball launching it with 45° trajectories to make maximize range. The motors are wrapped in rubber to increase friction with the ball, giving it a higher initial velocity.

D. Propulsion

Using two T200 thrusters keeps provides our vehicle with omnidirectional movement capabilities, the system simple, while still providing all the required movements we need, and they are

powered by high-capacity LiPo batteries to achieve full thrust power.

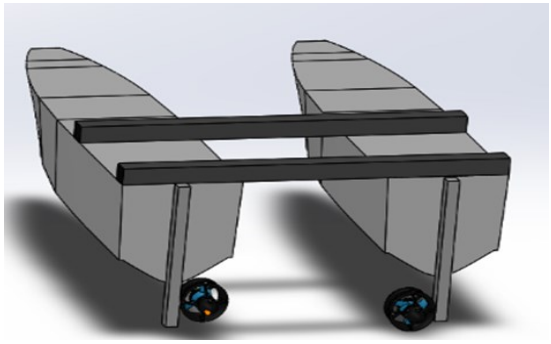

Figure 2: SolidWorks model of the hull structure with two rear-mounted T200 thrusters.

E. Electrical box

We used a transparent acrylic enclosure that contains all the ASV electrical units due to its light weightiness, simplicity to alter and manufacture, and cost. The reason to select acrylic material is to protect the units inside from water splashes created by high thrust functions, wind, and small waves. Through experience last year, the units were prone to degradation from splash water from high thrust functions, wind, and small waves.

These concerns are no longer present with this current design. The acrylic enclosure has a smooth surface that minimizes friction drag, hence improving hydro dynamical efficiency and power factor. Moreover, acrylic material enhances better cooling of units to reduce the threat of units overheating.

To freely allow safe operation of the ASV while providing ease of access and simplicity to carry out any modifications as well as debugging activities, the enclosure is sealed at the top via a hinged lid. It has dimensions of 60 × 25 × 15 cm with a thickness of 5mm to offer sufficient internal capacity and robustness to withstand minor injuries when competing.

SolidWorks model of the dual-hull vessel showing the ZED camera mounted on an aluminum beam structure above the hulls. The aluminum beams provide a rigid and stable mounting point for the camera, allowing a clear forward-facing field of view for visual perception tasks.

Figure 3: Electronic box with the main components: Jetson Tx2, Pixahawk, Arduino uno

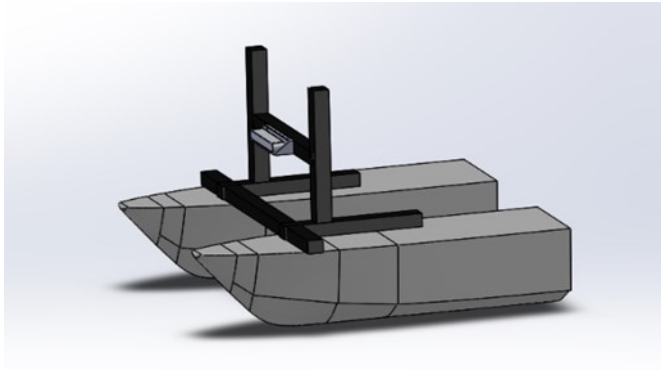

Figure 4: SolidWorks model of the 2-hulls with the ZED camera

F. Mechanisms (Ball Launcher, Water Pump)

The mechanism for delivering balls and water to the vessels around the course consists of three subsystems: the turret, the ball launcher, and the water cannon. By integrating these subsystems into a single assembly, we create a reliable method for aiming at targets.

1) Ball Launcher:

We designed our ball launcher by assembling two T200 thrusters horizontally and attaching rollers to them to grip and accelerate the balls between the rollers. We benefit from the T200 thrusters' high torque and speed to launch the balls efficiently.

Cylindrical tubes were added to guide the balls into and between the rollers; the inner diameter of the tubes is matched to the ball size, ensuring smooth delivery and reduced friction. Since we are using the same type of T200 thrusters as those

employed in our ASV's propulsion system, this simplifies the control system by allowing the use of shared motor controllers and software algorithms.

The motors are wrapped in rubber to increase friction with the ball, giving it a higher initial velocity.

2) Water Pump:

For water delivery, we are using a water pump with a flow rate of 2000 gallons per hour. It provides reliable and efficient water transfer while being easy to integrate into the ASV. We designed a nozzle to allow the water to be directed upward without the need to manually adjust its angle.

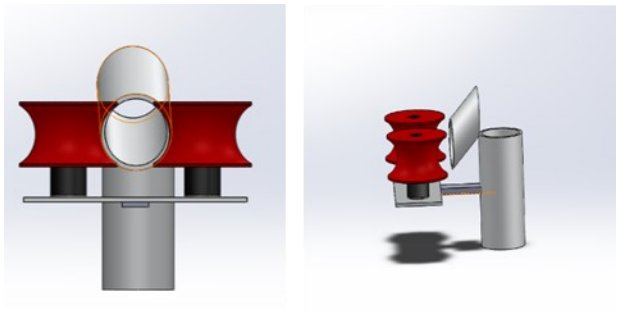

Figure 5: SolidWorks model of the ball launcher assembly, showing the roller mechanism and guiding tubes.

G. Electrical System

From previous years' participation, we gained confidence in our electrical system, as it proved its functionality and reliability. However, this season we decided to upgrade the power system due to new demands from upgraded or newly added hardware, such as 5G communication. Our approach was to use two LiPo batteries: one connected to the NVIDIA Jetson TX2, and the other connected to the thrusters and the remaining system components.

1) System Overview:

To protect the Jetson from overvoltage and sudden power interruptions, we have placed a UPS between the battery and the Jetson, ensuring stable and safe operation of the onboard computer. The E-stop allows us to safely stop the ASV system by cutting off all power to the system.

2) Battery Management System (BMS):

The power management system was designed to solve issues observed in previous iterations, where high current draw from the thrusters at full power caused voltage drops that affected other onboard devices. To prevent this, the system power is divided into three independent power lines, allowing each major subsystem to operate without interfering with the others.

A 24 V, 11 Ah LiPo battery is used to power the Jetson and Arduino through a USB power module, ensuring a stable supply for these sensitive components. Thruster power is provided by a dedicated 24 V, 15 Ah LiPo battery connected through a step-down converter, allowing the thrusters to draw high current without impacting the rest of the system.

A second 24 V, 15 Ah LiPo battery supplies the access point, water pump, and shooting mechanism, also regulated through a step-down converter. By separating high-current loads from current-sensitive electronics, this setup minimizes voltage fluctuations and improves overall system reliability. This approach allows the vehicle to achieve maximum thrust and performance while maintaining stable operation across all onboard devices.

3) Power-Stop Implementation:

The system employs both physical and electronic power kill mechanisms. The physical kill switch is a manually operated 3-to-3 port switch (Red Emergency Push-Button) that disconnects the three primary power lines of the vessel.

The electronic kill switch is controlled by an Arduino and triggered via a joystick command. While an RMV4 relay was initially used to interrupt system power, it proved unsuitable for the high current demands of the thrusters.

A high-current cutout was therefore added as an intermediate stage. The relay now controls the cutout, which safely disconnects the batteries from the system upon receiving a kill signal. Each battery has an independent cutout, all driven by a common relay control signal.

H. Software System Architecture

This year, we prioritized a simple and reliable software architecture built on ROS with a modular, node-based design. A dedicated Task Manager node serves as the high-level state machine, responsible for selecting and activating tasks, tracking the currently active task, and monitoring task success or failure. Each mission objective is implemented as an independent ROS node containing only the logic required to complete that specific task, reducing coupling and improving system robustness.

To further minimize complexity, we intentionally avoided full localization and mapping. Instead, Return-to-Launch (RTL) is handled through MAVROS, augmented with lightweight obstacle avoidance logic during the return phase. The Task Manager continuously monitors a global recall signal generated by an onboard audio detection module; when a specific frequency sound is detected during any task, the Task Manager immediately aborts all active tasks and commands the Pixhawk flight controller to execute an RTL maneuver, ensuring rapid and safe system recovery.

Computer vision and distance estimation are performed within ROS using a ZED camera running on the Jetson platform, while low-level actuation—such as ball shooting or water splashing—is handled by an Arduino connected to the Jetson. This clear separation between high-level perception and decision-making and low-level real-time control enables efficient processing, improved reliability, and predictable system behavior.

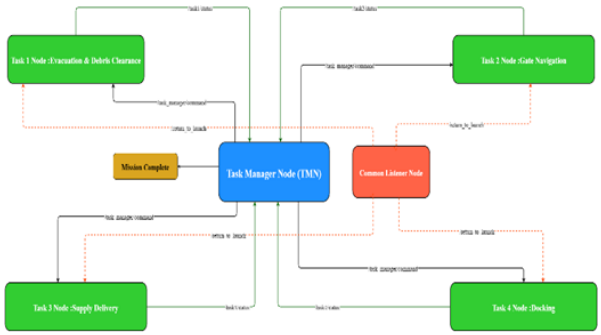

Figure 6: ROS node communication showing the Task Manager coordinating detection, navigation, delivery, and docking tasks.

III. Testing Strategy

From our experience last year, we learned that testing individual tasks alone was not enough to ensure the reliability of the full ASV system. Many of the issues we faced only appeared when all subsystems were running together, especially in environments that differed from our lab setup. As a result, this year we focused more on using simulation to understand system behavior early and to identify system failures before the competition.

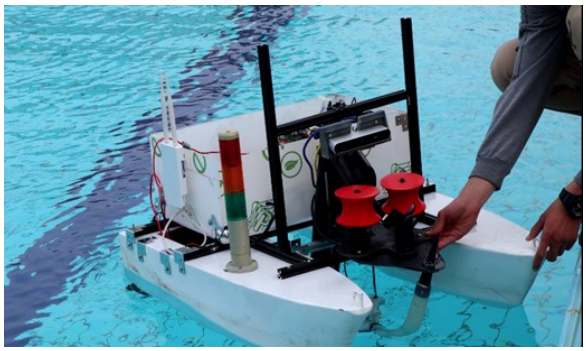

Figure 7: The ASV in the pool during testing, showing the ball launcher and water delivery system setup.

Power management was another major challenge in last year's system. We used sulfuric acid batteries (CP 1250HC), which were unable to supply the high current required by the T200 thrusters. During operation, the batteries showed voltage drops, causing the system to reset or shut down, especially during tasks require high power like the Speed Challenge.

At the time, power consumption was assumed to be ideal in the indoor tests. This year, we improved our approach by modeling realistic thruster loads and observing their impact on the simulation tests. Based on the test results, we switched to lithium-polymer (LiPo) batteries for both the thrusters and the rest of the onboard electronics. This change greatly improved voltage stability and allowed the ASV to operate reliably under high load conditions.

Although several ROS-based software modules were developed last year, we were unable to test the full autonomy tasks in sequence.

Due to task dependencies, each node was tested individually, but the complete mission was never tried before competition.

This year, simulation played a key role in detecting this problem. We tested the full ROS stack running, allowing tasks to run in the expected sequence during competition. This approach exposed issues such as timing mismatches, improper state transitions, and data synchronization problems. By identifying and fixing these issues in simulation, we were able to improve system stability before physical testing.

Overall, simulation helped us turn last year's setbacks into valuable learning opportunities. By testing our communication, power, and software systems under more realistic conditions, we were able to detect problems earlier and make informed design improvements. These changes resulted in a more reliable and competition-ready ASV, and they reinforced the importance of system-level testing alongside individual tasks validation.

ACKNOWLEDGMENT

The MW team's achievements and the successful upgrade of our Autonomous Surface Vehicle (ASV) would not have been possible without the motivation and generous financial support of the Military Technical College. We would like to extend our sincere appreciation to Brigadier General Hossam Ragheb and Captain Adel Mohab for their invaluable advice, guidance, and continuous support throughout the upgrade.

We are also deeply grateful to the Marine Engineering Department for providing specialized tools, technical expertise, and essential knowledge that greatly contributed to our development process. In addition, we acknowledge the Military Technical College for facilitating access to various locations and diverse environments that enabled comprehensive testing and validation of the ASV.

Finally, we would like to thank all the cadets for their valuable feedback, and practical suggestions, which played an important role in refining and improving our system.

REFERENCES

[1] K. Nonami, F.Kendoul, S.Suzuki, W. Wang, D. Nakazawa (2010) Autonomous Flying Robots for Unmanned Aerial Vehicles and Micro Aerial Vehicles.

[2] Team Handbook - RoboBoat 2026

[3] Ardupilot, "Mission Planner," Ardupilot, 2023.https://ardupilot.org/planner

[4] "ROS Documentation", OSRF. Available: http://wiki.ros.org/Documentation.

[5] L. Joseph, Mastering ROS for Robotics Programming, 2nd ed. Birmingham, UK: Packt Publishing, 2018.

[6] GitHub, "YOLOv4-Tiny · GitHub topics," GitHub. [Online]. Available: https://github.com/topics/yolov4-tiny

[7] mavlink, "MAVROS: MAVLink to ROS gateway," GitHub. [Online]. Available: https://githubgithub.com/mavlink/mavros.

[8] R. Szeliski, Computer Vision: Algorithms and Applications. New York, NY, USA: Springer, 2010.

APPENDIX A

SOFTWARE TESTING

Based on the lessons learned and shortcomings identified during the previous year, despite the system being nearly fully assembled and ready for deployment, we chose to conduct extensive simulations using Gazebo 11 to test and validate the software while minimizing unnecessary stress on the hardware components.

Each task was initially tested individually to ensure that every software module performed its intended function efficiently and reliably. One of the primary challenges encountered during simulation was accurately modeling the environmental variability present in the real competition course, as well as estimating appropriate hydrodynamic parameters for realistic vehicle behavior.

Figure 8: Testing the gate pass

Following individual task validation, the tasks were progressively integrated to verify that the complete software system could operate cohesively and accomplish all mission objectives. After completing the simulations and identifying optimal configurations in Gazebo, the required modifications were implemented in the final system design.

APPENDIX B

MECHANICAL TESTING

ANSYS was used to perform a computational fluid dynamics (CFD) analysis of the ASV hull in order to evaluate its hydrodynamic performance prior to physical testing. The simulation domain was defined to represent a water course, and the ASV hull geometry was placed within the flow field to analyze water–hull interaction under forward motion.

Velocity and flow contour were rendered for illustrating flow distribution around the hull, which is obtained from simulation results. These contours illustrate areas of higher flow velocity and wake development aft of the vehicle to help identify drag creating regions and general flow characteristics.

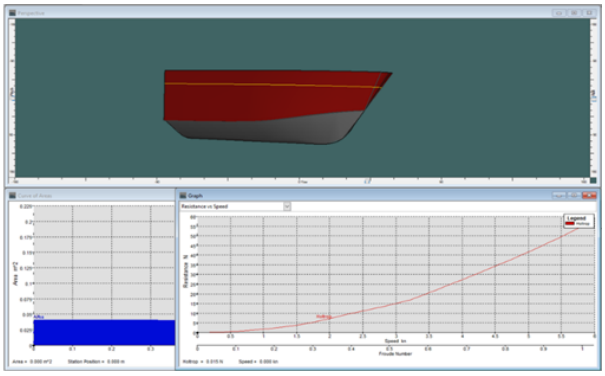

Figure 9: ASV hull model and resistance versus speed results obtained from hydrodynamic simulation

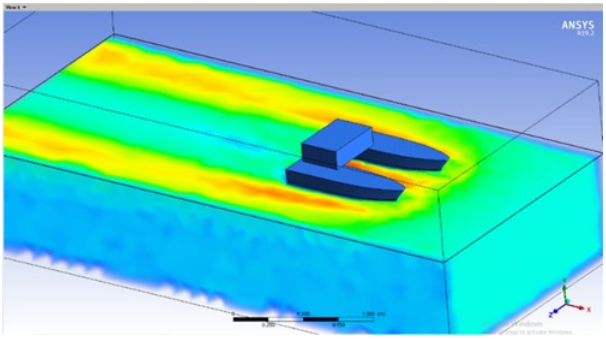

Figure 10 : Water flow simulation around the ASV hull showing velocity distribution and wake formation

Additionally, ANSYS was used to compute the resistance force acting on the hull at varying speeds. The resulting resistance-versus-speed curve demonstrates the expected nonlinear increase in

hydrodynamic resistance with velocity. This analysis was essential for estimating drag characteristics and validating the hull design for efficient operation.

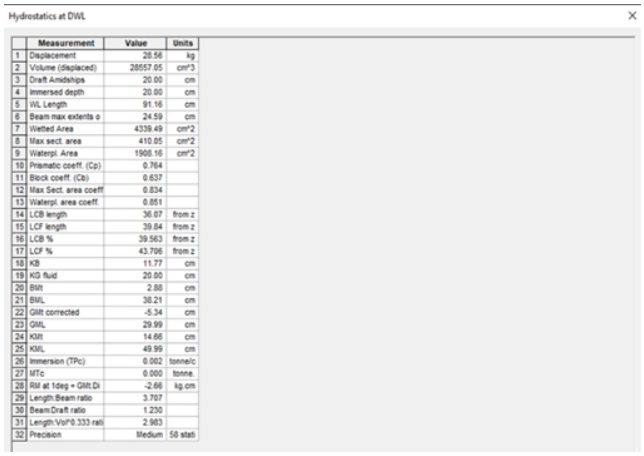
Hydrostatics at DWL

	Measurement	Value	Units
1	Displacement	28.56	kg
2	Volume (displaced)	28557.05	cm^3
3	Draft Amidships	20.00	cm
4	Immersed depth	20.00	cm
5	WL Length	91.16	cm
6	Beam max extents o	24.59	cm
7	Wetted Area	4339.49	cm^2
8	Max sect. area	410.05	cm^2
9	Waterpl. Area	1908.16	cm^2
10	Prismatic coeff. (Cp)	0.764	
11	Block coeff. (Cb)	0.637	
12	Max Sect. area coeff	0.834	
13	Waterpl. area coeff.	0.851	
14	LCB length	36.07	from z
15	LCF length	39.84	from z
16	LCB %	39.563	from z
17	LCF %	43.706	from z
18	KB	11.77	cm
19	KG fluid	20.00	cm
20	BMt	2.88	cm
21	BML	38.21	cm
22	GMt corrected	-5.34	cm
23	GML	29.99	cm
24	KMt	14.66	cm
25	KML	49.99	cm
26	Immersion (TPc)	0.002	tonne/c
27	MTc	0.000	tonne
28	RM at 1deg = GMt.Di	-2.66	kg.cm
29	Length:Beam ratio	3.707	
30	Beam:Draft ratio	1.230	
31	Length:Vol^0.333 rati	2.983	
32	Precision	Medium	58 stati

Figure 11: Hydrostatic properties of the ASV hull at the design waterline (DWL) obtained from the hull analysis tool.

Hydrostatic analysis was done to check the basic physical and stability characteristics of the ASV hull at the Design Waterline (DWL). For this, main parameters like displacement (28.56 kg), immersed volume (28,557 cm^3), and draft (20 cm) were calculated, which confirmed that the hull could not only bear the weight of the vehicle but also provide the required buoyancy.

Besides supporting the simulations of the hydrodynamics and the design of the control system, this hydrostatics report was also a very important input in the whole process and it made sure that ASV would have the three features of being buoyant, stable, and maneuverable under operation.

The outcomes of the ANSYS simulations were used to support the selection of hydrodynamic parameters and to inform performance expectations in the Gazebo simulation and control system design. Conducting this analysis in simulation reduced development risk and minimized unnecessary hardware iterations.

The hull lines plan shows the ASV's shape from three key views: the body plan displays cross-sectional shapes of the hull at different points, revealing its underwater volume and symmetry; the half-breadth plan provides a top-down outline of the hull sections, illustrating beam changes and helping analyze resistance; and the sheer plan presents the side profile, showing the hull's longitudinal curves above and below the waterline, which affect wave-making and stability. Together, these views give a complete picture of the hull's form, essential for understanding its buoyancy, stability, and hydrodynamic performance.

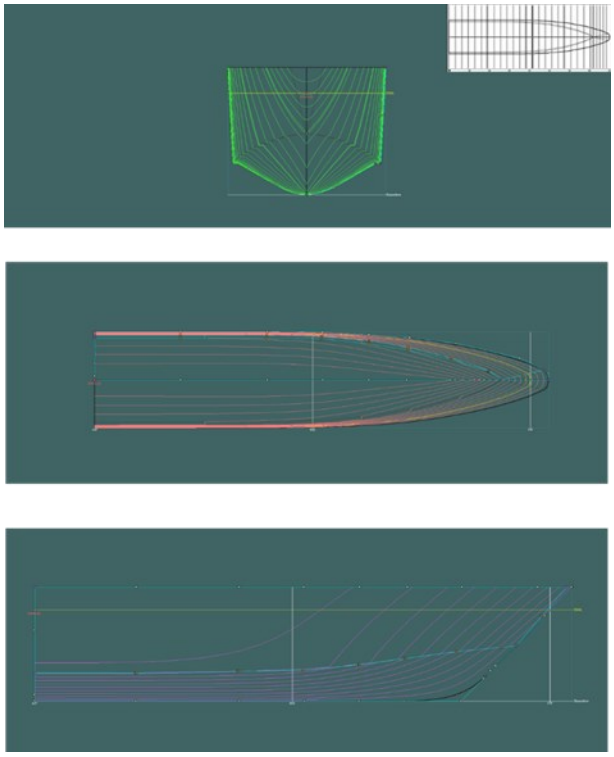
Figure 12: Body plane, water lines, and buttocks of the hulls.

APPENDIX C

BALL SHOOTING CALCULATIONS

As seen in Figure 5, the ball launcher mechanism is made up of two rubber-coated T200 thrusters that are positioned horizontally and function as rollers. Before being released, the ball is accelerated by frictional contact between the two rotating rollers. The arrangement of the symmetric rollers guarantees:

1. The ball's balanced normal forces
2. At launch, there is slight lateral deviation
3. Stable and repeatable ball exit setup

The launcher is positioned on the ASV so that the ball exits at a height of about 0.20 meters above the water's surface.

The competition JBM Squash Ball with the following parameters:

Radius = $Radius = \mathrm{r} = 0.0275\ \mathrm{m}$
Mass = $m = 0.024\ kg$
Cross-sectional Area = A =
$\pi = \pi r^2 \times 0.0275^2 = 2.38 \times 10^{-3}\ m^2$

The following assumptions are considered:

1. The ball is considered as a rigid sphere.
2. The angle of launch is near horizontal.
3. The rollers achieve a constant angular speed prior to the release of a ball.
4. The rubber coating ensures dominant static friction.
5. Air resistance is governed by a quadratic drag model.
6. Effects of wind and water splash are neglected.
7. Ball deformation is small and is not dominant in the energy losses.

From manufacturer data:
RPM ≈ 5300

$$\omega = \frac{2\pi \cdot \mathrm{RPM}}{60} = \approx 555\ \mathrm{rad/s}$$

roller contact radius $= r_c \approx 0.03$

Tangential surface velocity $= v_{roller}$

$$v_{roller} = wr_c = 555 \times 0.03 \approx 16.7\ \frac{m}{s}$$

Accounting for frictional losses, compliance, and minor slip, the best-case practical ball exit velocity is c estimated as:

$$time\ of\ flight = \sqrt{\frac{2h}{g}} \approx 0.2\mathrm{s}$$

Air resistance is modeled using quadratic drag, appropriate for a spherical object:

$$F_d = \frac{1}{2}\rho C_d A v^2$$

Where:

$$\rho = 1.225\ \frac{\mathrm{kg}}{m^3}$$

$$C_d = 0.47$$

At best- case velocity:

$$F_d \approx 0.098\ \mathrm{N}$$

Corresponding horizontal deceleration:

$$a_d = \frac{F_d}{m} \approx 4.1\ \frac{\mathrm{m}}{s^2}$$

Velocity loss during flight:

$$\Delta v = \frac{a_d}{t} = 4.1 \times 0.20 = 0.82\ \frac{\mathrm{m}}{s}$$

Average horizontal velocity:

$$v_{avg} = v_0 - \frac{\Delta v}{2} = 12 - 0.41 = 11.59\ \frac{\mathrm{m}}{s}$$

Best-Case Horizontal Range (With Drag):

$$R_{best} = v_{avg} t = 11.59 \times 0.20 \approx 2.32\ \mathrm{m}$$

Based on projectile motion and drag analysis, a maximum theoretical range of about 2.3 m can be obtained using the ball launcher; thus, targets should be within a range of 2.0 m or less to maximize ball delivery. An optimal engagement window: 1.8 m – 2.2m

APPENDIX D

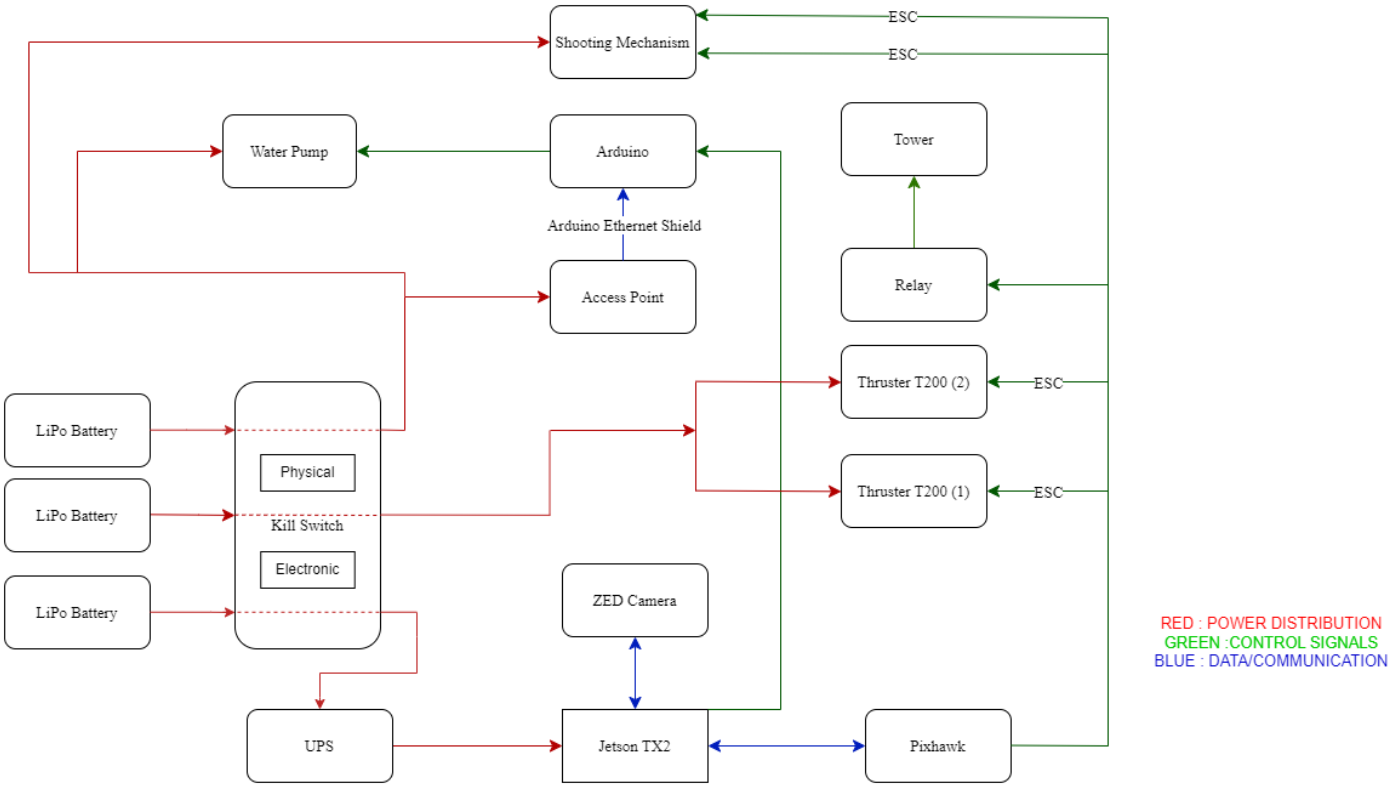

Figure 13: Electrical System Diagram.